HHS Public Access

Author manuscript

Math Biosci. Author manuscript; available in PMC 2017 December 11.

Published in final edited form as:

Math Biosci. 2017 May ; 287: 93–104. doi:10.1016/j.mbs.2016.09.013.

Evaluating targeted interventions via meta-population models with multi-level mixing

Zhilan Feng[1], **Andrew N. Hill**[2], **Aaron T. Curns**[3], and **John W. Glasser**[3]

[1]Department of Mathematics, Purdue University, West Lafayette, Indiana

[2]National Center for HIV/AIDS, Viral Hepatitis, STD, and TB Prevention, CDC, Atlanta, Georgia

[3]National Center for Immunization and Respiratory Diseases, CDC, Atlanta, Georgia

Abstract

Among the several means by which heterogeneity can be modeled, Levins' (1969) meta-population approach preserves the most analytical tractability, a virtue to the extent that generality is desirable. When model populations are stratified, contacts among their respective sub-populations must be described. Using a simple meta-population model, Feng et al. (2015) showed that mixing among sub-populations, as well as heterogeneity in characteristics affecting sub-population reproduction numbers, must be considered when evaluating public health interventions to prevent or control infectious disease outbreaks. They employed the convex combination of preferential within- and proportional among-group contacts first described by Nold (1980) and subsequently generalized by Jacquez et al. (1988). As the utility of meta-population modeling depends on more realistic mixing functions, the authors added preferential contacts between parents and children and among co-workers (Glasser et al. 2012). Here they further generalize this function by including preferential contacts between grandparents and grandchildren, but omit workplace contacts. They also describe a general multi-level mixing scheme, provide three two-level examples, and apply two of them. In their first application, the authors describe age- and gender-specific patterns in face-to-face conversations (Mossong et al. 2008), proxies for contacts by which respiratory pathogens might be transmitted, that are consistent with everyday experience. This suggests that meta-population models with inter-generational mixing could be employed to evaluate prolonged school-closures, a proposed pandemic mitigation measure that could expose grandparents, and other elderly surrogate caregivers for working parents, to infectious children. In their second application, the authors use a meta-population SEIR model stratified by 7 age groups and 50 states plus the District of Columbia, to compare actual with optimal vaccination during the 2009–10 influenza pandemic in the United States. They also show that vaccination efforts could have been adjusted month-to-month during the fall of 2009 to ensure maximum impact. Such applications inspire confidence in the reliability of meta-population modeling in support of public health policymaking.

Correspondence: Dr. John Glasser; 1600 Clifton Road, NE; Mail Stop A-34; Atlanta, GA 30333 USA; +1-404-639-8780 (voice); +1-404-315-2493 (facsimile); jglasser@cdc.gov.

Conflicts: The authors declare that they have no conflicts of interest.

Disclaimer: The findings and conclusions in this report are those of the authors and do not necessarily represent the official position of the Centers for Disease Control and Prevention or other institutions with which they are affiliated.

Keywords

meta-population modeling; mixing functions; designing or evaluating public health interventions

1. Introduction

Agent-based, network and population models each have features that, for particular applications, make one the obvious choice. For others, identifying the best approach involves weighing their respective strengths and weaknesses. While each can incorporate structural heterogeneity, agent-based and meta-population modeling sacrifice and preserve, respectively, the most analytical tractability. As analyses invariably increase understanding, we seek to augment the usefulness of systems of weakly coupled large sub-populations, or meta-populations (Levins 1969), in modeling the spread of pathogens, arguably the most important of several challenges that Ball et al. (2015) describe.

In consolidating and extending earlier contributions to our understanding of the impact of heterogeneity (in characteristics affecting sub-population reproduction numbers) and non-random mixing, Feng et al. (2015) used a convex combination of preferential within- and proportional among-group contacts (Jacquez et al. 1988). In that mixing function, the fraction of within-group contacts and their complements correspond to Ball et al.'s (2015) coupling strength, which determines location on a continuum whose limiting meta-populations behave as one or as multiple independent sub-populations. The simplicity of this function facilitates theoretical studies, but it is too simple for most applications.

Accordingly, we generalized the function of Jacquez et al. (1988) by including preferential contacts between parents and children and among co-workers as well as contemporaries (Glasser et al. 2012). Here we include grandparents and grandchildren, but omit co-workers. Together with observations from a study of face-to-face conversations, a proxy for contacts by which the pathogens causing respiratory diseases might be transmitted (Mossong et al. 2008), this new function permits us to describe mixing patterns within and between genders by age. Motivated by the consistency of results with everyday human experience, we develop a formal multi-level mixing scheme.

We present several two-level examples and show that modeling influenza by age and gender or location could inform pandemic mitigation efforts. Our first application aims to facilitate reevaluating the impact of prolonged school closures, which could increase mortality among grandparents and other elderly surrogates for working parents, and second to assist in optimally allocating available vaccine among groups (Feng et al. 2015), a recurring theme with respect to influenza. As public health resources invariably are limited, other potential applications of our approach abound.

2. Methods

Mixing is inconsequential only in homogeneous populations. Feng et al. (2015) show that heterogeneity in factors affecting sub-population reproduction numbers increases the meta-population reproduction number even if mixing is random, and that non-random mixing

increases it further, especially if heterogeneous. Accordingly, meta-population models must specify the manner in which sub-population members mix (i.e., proportionally or preferentially, and if the latter, how).

2.1 Theory

Busenberg and Castillo-Chavez (1991) define c_{ij} as proportions of contacts members of group i have with group j, given that i has contacts. Their criteria that mixing functions should meet are:

1. $c_{ij} \geq 0,$
2. $\sum_{j=1}^{k} c_{ij}=1, i=1, \ldots, k,$ and
3. $a_i N_i c_{ij}=a_j N_j c_{ji},$

where the N_i are group sizes and a_i are average *per capita* contact rates of groups $i = 1, \ldots, k$, called activities. Formulae derivable from these conditions follow.

2.1.1 A Simple Function—If a proportion ε_i of i-group contacts is reserved for others in group i, called preference, and the complement $(1–\varepsilon_i)$ is distributed among all groups, including i, via the proportional mixing formula, $a_i N_i / \sum_j a_j N_j$, then the fractions of their contacts that members of group i have with members of groups j are

$$c_{ij}=\varepsilon_i \delta_{ij}+(1-\varepsilon_i)\frac{(1-\varepsilon_j)\, a_j N_j}{\sum_k (1-\varepsilon_k)\, a_k N_k},$$

where δ_{ij} is the Kronecker delta (i.e., $\delta_{ij} = 1$ if $i = j$ and $\delta_{ij} = 0$ if $i \neq j$). Jacquez and colleagues (1988) obtained this expression by allowing the fraction of within-group contacts, ε, to vary among groups in Nold's (1980) preferred mixing function.

2.1.2 One-Level Mixing—When groups are age classes, Glasser et al. (2012) generalized this function to contacts between parents and children and among co-workers as well as contemporaries. Here we add a second generation (i.e., grandchildren and grandparents, another set of sub- and super-diagonals). For simplicity, we omit contacts among co-workers and assume that generation time, G (average age of women at the birth of their daughters) and longevity, L (average expectation of life at birth or age at death) are constant. Then the fractions of their contacts that members of group i have with members of group j may be defined as

$$c_{ij}:=\phi_{ij}+(1-\sum_{s=1}^{5}\varepsilon_{si})f_j, f_j:=\frac{(1-\sum_{s=1}^{5}\varepsilon_{sj})a_j N_j}{\sum_{k=1}^{n}(1-\sum_{s=1}^{5}\varepsilon_{sk})a_k N_k},$$

where the ε_{si} are fractions of contacts reserved for the s^{th} sub-population, $s = 1, \ldots, 5$ (contemporaries, parents, children, grandparents, and grandchildren), and a_i and N_i are the *per capita* contact rates and sizes of the i^{th} age group, $i = 1, \ldots, n$. Because people whose ages equal or exceed G but are less than $2G$ may have children, but not grandchildren; people whose ages equal or exceed $2G$ can have both children and grandchildren; people whose ages are less than or equal to $L–2G$ may have parents and grandparents; people whose ages are less than or equal to $L–G$ may have parents, but not grandparents; and those whose ages are between $2G$ and $L–2G$ may have children, grandchildren, parents and grandparents; we define ϕ_{ij} as

$$\phi_{ij} := \begin{cases} \delta_{ij}\varepsilon_{1i} + \delta_{i(j+G)}\varepsilon_{2i}, & G \le i < 2G, \\ \delta_{ij}\varepsilon_{1i} + \delta_{i(j+G)}\varepsilon_{2i} + \delta_{i(j+2G)}\varepsilon_{4i}, & i \ge 2G, \\ \delta_{i(j-2G)}\varepsilon_{5i} + \delta_{i(j-G)}\varepsilon_{3i} + \delta_{ij}\varepsilon_{1i}, & i \le L - 2G, \\ \delta_{i(j-G)}\varepsilon_{3i} + \delta_{ij}\varepsilon_{1i}, & L - 2G < i \le L - G \end{cases}.$$

If age groups are 0–4, 5–9, … and the generation time is 25 years, by $i > G$ we mean age greater than class 5. Thus,

$$\delta_{ij} = \begin{cases} 1 \text{ if } i = j \\ 0 \text{ otherwise} \end{cases}, \ \delta_{i(j\pm G)} = \begin{cases} 1 \text{ if } i = j \pm G \\ 0 \text{ otherwise} \end{cases} \text{ and } \delta_{i(j\pm 2G)} = \begin{cases} 1 \text{ if } i = j \pm 2G \\ 0 \text{ otherwise} \end{cases}.$$

To satisfy Busenberg's and Castillo-Chavez' (1991) third condition (that contacts must balance), the non-zero elements of $\vec{\varepsilon}_2 ; \text{and} ; \vec{\varepsilon}_3$ and of $\vec{\varepsilon}_4 ; \text{and} ; \vec{\varepsilon}_5$ must be related. Again, if age groups are 0–4, 5–9, … and the generation time is 25 years, $a_i \times N_i \times \varepsilon_{4i} = a_j \times N_j \times \varepsilon_{5j}$, for $i = 11, 12, \ldots, n$ and $j = i–2G$. This ensures that $a_i \times N_i \times c_{ij} = a_j \times N_j \times c_{ji}$ for $j = i–2G$. Note also that $0 \le \sum_{s=1}^{5} \varepsilon_{si} \le 1$.

2.1.3 Multiple-Level Mixing—Some applications require multiple strata. Beginning with two, consider m sub-populations (e.g., locations or genders) and n classes (e.g., age or activity groups). Let l_i denote the i^{th} location (l for location) and a_j denote the j^{th} age group (a for age), $1 \le i \le m$ and $1 \le j \le n$. We use this compound notation whenever indices might otherwise be confused.

Let $A_{l_i a_j}$ denote the activity, or average *per capita* contact rate, of individuals at location l_i and age a_j and $N_{l_i a_j}$ denote the number of people at location l_i of age a_j. Then the probability of contact between persons in location l_i, age a_j and location l_p, age a_q may be described by a matrix with entries

$$c_{l_i a_j l_p a_q} := \varepsilon_{l_i a_j}\delta_{l_i l_p}\delta_{a_j a_q} + (1 - \varepsilon_{l_i a_j}) f_{l_p a_q}, \ \ 1 \le i, p \le m, \ \ 1 \le j, q \le n,$$

where

$$f_{l_p a_q} := \frac{(1 - \varepsilon_{l_p a_q}) A_{l_p a_q} N_{l_p a_q}}{\sum_{j=1}^{n}\sum_{i=1}^{m} (1 - \varepsilon_{l_i a_j}) ; A_{l_i a_j} N_{l_i a_j}}.$$

In these expressions, $\varepsilon_{l_i a_j}$ represents preference for one's own age/location group, δ_{rs} is the Kronecker delta function, taking values of 1 (if $r = s$) or 0 (if $r \neq s$), and $f_{l_p a_q}$ is random mixing (i.e., proportional to contacts, $A_{l_p a_q} N_{l_p a_q}$). For some applications, however, mixing among ages and locations (or other strata) are independent (e.g., members of an age class may contact others of the same age preferentially regardless of their location, gender or any other discrete characteristic).

Letting $\varepsilon^{(l)}_{l_i a_j}$ and $\varepsilon^{(a)}_{l_i a_j}$ represent preferences for one's own location and age class, respectively, matrix entries become

$$\begin{aligned} c_{l_i a_j l_p a_q}: \\ &= \varepsilon^{(l)}_{l_i a_j} \delta_{l_i l_p} \left[\varepsilon^{(a)}_{l_i a_j} \delta_{a_j a_q} + (1 - \varepsilon^{(a)}_{l_i a_j}) F_{l_i a_q} \right] \\ &+ (1 - \varepsilon^{(l)}_{l_i a_j}) \left[\varepsilon^{(a)}_{l_i a_j} \delta_{a_j a_q} G_{l_p a_q} + (1 - \varepsilon^{(a)}_{l_i a_j}) H_{l_p a_q} \right], \quad 1 \leq i, p \leq m, \quad 1 \leq j, q \leq n, \end{aligned}$$

where

$$F_{l_i a_q} = \frac{\left[1 - \varepsilon^{(a)}_{l_i a_q}\right] A_{l_i a_q} N_{l_i a_q}}{\sum_k \left[1 - \varepsilon^{(a)}_{l_i a_k}\right] A_{l_i a_k} N_{l_i a_k}}, G_{l_p a_q} = \frac{\left[1 - \varepsilon^{(l)}_{l_p a_q}\right] A_{l_p a_q} N_{l_p a_q}}{\sum_r \left[1 - \varepsilon^{(l)}_{l_r a_q}\right] A_{l_r a_q} N_{l_r a_q}},$$

$$\text{and} \quad H_{l_p a_q} = \frac{\left[1 - \varepsilon^{(a)}_{l_p a_q}\right] \left[1 - \varepsilon^{(l)}_{l_p a_q}\right] A_{l_p a_q} N_{l_p a_q}}{\sum_r \sum_k \left[1 - \varepsilon^{(a)}_{l_r a_k}\right] \left[1 - \varepsilon^{(l)}_{l_r a_k}\right] A_{l_r a_k} N_{l_r a_k}}.$$

In this expression for $c_{l_i a_j l_p a_q}$, the terms in square brackets represent age-preferential mixing in one's own and other locations, respectively, and $F_{l_p a_q}$, $G_{l_p a_q}$, and $H_{l_p a_q}$ represent proportional mixing with respect to age, location, and both.

Checking to ensure that $\sum_{p=1}^{m} \sum_{q=1}^{n} c_{l_i a_j l_p a_q} = 1$ for any given *i* and *j*, we find that

$$\begin{aligned} \sum_{p=1}^{m} \sum_{q=1}^{n} \varepsilon^{(l)}_{l_i a_j} \delta_{l_i l_p} \left[\varepsilon^{(a)}_{l_i a_j} \delta_{a_j a_q} + (1 - \varepsilon^{(a)}_{l_i a_j}) F_{l_i a_q} \right] &= \varepsilon^{(l)}_{l_i a_j} \left[\varepsilon^{(a)}_{l_i a_j} + (1 - \varepsilon^{(a)}_{l_i a_j}) \sum_q F_{l_i a_q} \right] = \varepsilon^{(l)}_{l_i a_j}, \sum_{p=1}^{m} \sum_{q=1}^{n} \left[\varepsilon^{(a)}_{l_i a_j} \delta_{a_j a_q} G_{l_p a_q} + (1 - \varepsilon^{(a)}_{l_i a_j}) H_{l_p} \right. \\ = \sum_{p=1}^{m} \varepsilon^{(a)}_{l_i a_j} G_{l_p a_j} \\ + \sum_{p=1}^{m} \sum_{q=1}^{n} (1 - \varepsilon^{(a)}_{l_i a_j}) H_{l_p a_q} = 1. \end{aligned}$$

We can also verify that the constraint

$$A_{l_i a_j} N_{l_i a_j} c_{l_i a_j l_p a_q} = A_{l_p a_q} N_{l_p a_q} c_{l_p a_q l_i a_j}, \quad i \neq p, \quad j \neq q,$$

is satisfied:

$$\begin{aligned} A_{l_i a_j} N_{l_i a_j} c_{l_i a_j l_p a_q} &= A_{l_i a_j} N_{l_i a_j} (1 - \varepsilon^{(l)}_{l_i a_j})(1 - \varepsilon^{(a)}_{l_i a_j}) H_{l_p a_q} \\ = A_{l_i a_j} N_{l_i a_j} (1 - \varepsilon^{(l)}_{l_i a_j})(1 - \varepsilon^{(a)}_{l_i a_j}) &\frac{(1-\varepsilon^{(a)}_{l_p a_q})(1-\varepsilon^{(l)}_{l_p a_q}) A_{l_p a_q} N_{l_p a_q}}{\sum_r \sum_k \left[1 - \varepsilon^{(a)}_{l_r a_k}\right] \left[1 - \varepsilon^{(l)}_{l_r a_k}\right] A_{l_r a_k} N_{l_r a_k}} \end{aligned}$$

and

$$\begin{aligned} A_{l_p a_q} N_{l_p a_q} c_{l_p a_q l_i a_j} &= A_{l_p a_q} N_{l_p a_q} (1 - \varepsilon^{(a)}_{l_p a_q})(1 - \varepsilon^{(l)}_{l_p a_q}) H_{l_i a_j} \\ = A_{l_p a_q} N_{l_p a_q} (1 - \varepsilon^{(a)}_{l_p a_q})(1 - \varepsilon^{(l)}_{l_p a_q}) &\frac{(1-\varepsilon^{(l)}_{l_i a_j})(1-\varepsilon^{(a)}_{l_i a_j}) A_{l_i a_j} N_{l_i a_j}}{\sum_r \sum_k \left[1 - \varepsilon^{(a)}_{l_r a_k}\right] \left[1 - \varepsilon^{(l)}_{l_r a_k}\right] A_{l_r a_k} N_{l_r a_k}}. \end{aligned}$$

Once we have an expression for $c_{l_i a_j l_p a_q}$that is suitable for our application, we can formulate the force or hazard rate of infection per susceptible person as

$$\lambda_{l_i a_j} = A_{l_i a_j} \beta_{l_i a_j} \sum_{p=1}^{m} \sum_{q=1}^{n} c_{l_i a_j l_p a_q} \left(\frac{I_{l_p a_q}}{N_{l_p a_q}} \right), \quad 1 \leq i \leq m, \quad 1 \leq j \leq n\,.$$

Two-Level Examples.

2.2.3.1 Age and Location: Proximity must affect inter-personal contacts in spatial meta-populations. Glasser et al. (2016) assumed that contacts among sub-populations at different locations were a negative exponential function of inter-location distances. Combining such spatial with age-dependent mixing, we define

$$c_{l_i a_j l_p a_q} := \frac{c^{(p)}_{a_j a_q} e^{-b d_{l_i l_p}}}{\sum_{r=1}^{n} \sum_{s=1}^{m} c^{(p)}_{a_j a_r} e^{-b d_{l_i l_s}}}, \; 1 \leq i, p \leq m, \text{ and } 1 \leq j, q \leq n,$$

$$\text{where } c^{(p)}_{a_j a_q} = \varepsilon_{a_j} \delta_{a_j a_q} + (1 - \varepsilon_{a_j}) F_{l_p a_q} \text{ and } \; F_{l_p a_q} = \frac{(1 - \varepsilon_{a_q}) A_{l_p a_q} N_{l_p a_q}}{\sum_{k=1}^{n} (1 - \varepsilon_{a_k}) A_{l_p a_k} N_{l_p a_k}}.$$

In these expressions, *b* is the rate at which contacts diminish with distance (which may depend on age, but if so, b_{a_j} ; and ; b_{a_q}must be averaged to satisfy the balance condition), $d_{l_i l_p}$ is the distance between locations *i* and *p*, $F_{l_p a_q}$corresponds to proportional mixing (with respect to age) of persons in group *q* at location *p*, ε_{a_q}denotes the fraction of contacts that

individuals aged q (at any location) reserve for others in the same group (preference), and $c^{(p)}_{a_j a_q}$ represents the fraction of their contacts that individuals aged j have with individuals aged a_q at location l_p. Because contacts must balance, $c^{(p)}_{a_j a_q} \times N_{l_p a_j} \times A_{l_p a_j} = c^{(p)}_{a_q a_j} \times N_{l_p a_q} \times A_{l_p a_q}$, the superscript can be dropped only if age group sizes are the same at all locations, i.e., $N_{l_i a_q} = N_{l_p a_q} = N_{a_q}$.

2.1.3.2 Immigrants and Natives: Consider the case of immigrant (l_1=1) and native populations (l_2=2), a distinction that may matter for models designed to evaluate interventions to mitigate diseases whose prevalence differs at home and abroad (e.g., tuberculosis). The preference for population 1 of individuals aged a_j in population 1 is $\varepsilon^{(l)}_{1a_j}$; similarly, the preference for population 2 of individuals in population 2 is $\varepsilon^{(l)}_{2a_j}$.

If there is no age preference $(\varepsilon^{(a)}_{l_i a_j} = 0)$, the probability that individuals aged a_j in population 1 contact persons aged a_q in population 1 (note that $\delta_{1l_1} = 1$) is

$$c_{1a_j 1a_q} = \varepsilon^{(l)}_{1a_j} F_{1a_q} + (1 - \varepsilon^{(l)}_{1a_j}) H_{1a_q}$$
$$= \varepsilon^{(l)}_{1a_j} \frac{A_{1a_q} N_{1a_q}}{\sum_k A_{1a_k} N_{1a_k}} + (1 - \varepsilon^{(l)}_{1a_j}) \frac{\left[1 - \varepsilon^{(l)}_{1a_q}\right] A_{1a_q} N_{1a_q}}{\sum_r \sum_k \left[1 - \varepsilon^{(l)}_{l_r a_k}\right] A_{l_r a_k} N_{l_r a_k}}.$$

And the probability that individuals aged a_j in population 1 contact persons aged a_q in population 2 (note that $\delta_{1l_2} = 0$) is

$$c_{1a_j 2a_q} = (1 - \varepsilon^{(l)}_{1a_j}) H_{2a_q} = (1 - \varepsilon^{(l)}_{1a_j}) \frac{\left[1 - \varepsilon^{(l)}_{2a_q}\right] A_{2a_q} N_{2a_q}}{\sum_r \sum_k \left[1 - \varepsilon^{(l)}_{l_r a_k}\right] A_{l_r a_k} N_{l_r a_k}}.$$

2.1.3.3 Sexual Contacts: Another case with m = 2 is age- or activity-stratified mixing between females (l_1=1) and males (l_2=2), most of whose contacts are reserved for members of the other gender. (Replacing age with sexual activity, the groups might comprise sex workers and their clients.)

If contacts are entirely heterosexual, $\varepsilon^{(l)}_{1a_j} = \varepsilon^{(l)}_{2a_q} = 0, \;\; 0 \le \varepsilon^{(a)}_{1a_j}, \;\; \varepsilon^{(a)}_{2a_q} < 1, \;\; j, q = 1, \ldots, n.$ Thus, F is irrelevant. And, if there are no contacts within l_1 and l_2, the denominator in G should not be a sum, whereupon G = 1. Similarly, the sum over r in the denominator of H should be omitted. That is,

$$G_{1a_q} = G_{2a_q} = 1, \text{ and } ; H_{2a_q} = \frac{\left[1 - \varepsilon^{(a)}_{2a_q}\right] A_{2a_q} N_{2a_q}}{\sum_k \left[1 - \varepsilon^{(a)}_{2a_k}\right] A_{2a_k} N_{2a_k}},$$

whereupon

$$c_{1a_j 2a_q} = \varepsilon^{(a)}_{1a_j} \delta_{a_j a_q} + (1 - \varepsilon^{(a)}_{1a_j}) H_{2a_q}.$$

And the rate of infection for a female aged *j* is

$$\lambda_{1a_j} = \beta_{1a_j} A_{1a_j} \sum_{q=1}^{n} c_{1a_j 2a_q} \left(\frac{I_{2a_q}}{N_{2a_q}} \right).$$

2.2 Applications

In this section, we use two-level mixing functions, age with gender or location, in pandemic influenza applications, the first designed to facilitate deducing the impact of a proposed mitigation measure, prolonged school closures, and second to assist in optimally allocating available vaccine among groups.

2.2.1 Prolonged School Closures—In the best studies to date, modelers have assumed that mixing patterns during prolonged school closures would resemble those during weekends or school holidays. In many young families, however, both parents work, but not usually on weekends. And working parents plan activities for their children during holidays (e.g., sports and summer camps). Their options for unanticipated school closures are to miss work or – depending on their children's ages – to leave them at home alone or arrange for *ad hoc* child care. The first two options become less attractive the longer that schools are closed, leading to communal child care, mitigating the impact of school closures, or involving grandparents, potentially increasing morbidity if not mortality among the elderly. With our 5-diagonal mixing function, the net impact of prolonged school closures could be deduced more realistically than it has been heretofore.

Accordingly, we fit our function to observations by 5-year age class from the PolyMod study (Mossong et al. 2008) stratified by gender. If M_{1a_j} females (I_1=1) in age group *j* reported $C_{1a_j 1a_q}$face-to-face conversations with females in age group *q*, for example, one would calculate $A_{1a_j} = \sum_{q=1}^{n} C_{1a_j 1a_q} / M_{1a_j}$, their average *per capita* contact rates, and $c_{1a_j 1a_q} = C_{1a_j 1a_q} / A_{1a_j} M_{1a_j}$, fractions of their contacts that were with females in age group *q*. Female contacts with males (I_2=2) would be calculated similarly, as would male contacts with members of each gender.

2.2.1.1. Parameter estimates: Delta formulations are convenient mathematically, but probability density functions are more realistic (Hethcote 1996). Accordingly, when estimating parameters, we determine the ages of persons with whom contacts are preferential by fitting Gaussian kernels sampled at discrete points. That is, we replace the deltas in our 5-diagonal mixing function with

$$\varphi_{a_i a_j}=\frac{1}{\sqrt{2\pi}\sigma_{1i}}e^{-;\frac{[age(j)-age(i)]^2}{2\sigma_{1i}^2}},\ \varphi_{a_i a_{(j+G)}}=\frac{1}{\sqrt{2\pi}\sigma_{2i}}e^{-;\frac{[age(j)-age(i-G)]^2}{2\sigma_{2i}^2}},\ \varphi_{a_i a_{(j-G)}}=\frac{1}{\sqrt{2\pi}\sigma_{3i}}e^{-;\frac{[age(j)-age(i+G)]^2}{2\sigma_{3i}^2}},$$
$$\varphi_{a_i a_{(j+2G)}}=\frac{1}{\sqrt{2\pi}\sigma_{4i}}e^{-;\frac{[age(j)-age(i-2G)]^2}{2\sigma_{4i}^2}},\ \text{and}\ \varphi_{a_i a_{(j-2G)}}=\frac{1}{\sqrt{2\pi}\sigma_{5i}}e^{-;\frac{[age(j)-age(i+2G)]^2}{2\sigma_{5i}^2}},$$

where $\varphi_{a_i a_j}$, $\varphi_{a_i a_{(j+G)}}$, $\varphi_{a_i a_{(j-G)}}$, $\varphi_{a_i a_{(j+2G)}}$, and $\varphi_{a_i a_{(j-2G)}}$ allow persons aged a_i and those aged a_j, $a_{j\pm G}$, or $a_{j\pm 2G}$ to be contemporaries even if $a_i \neq a_j$, parents/children even if $|a_i - a_j| \neq G$, and grandparents/grandchildren even if $|a_i - a_j| \neq 2G$. Given this functional form, the variances determine if persons aged a_j are contemporaries, parents/children, or grandparents/grandchildren of those aged a_i.

We used *Mathematica*'s NMinimize function to estimate the generation time, G, the reserved fractions of contacts, ε_{sga}, and variances of the Gaussian kernels, σ_{sga}, for the $s = 1, \ldots, 5$ sub-populations, $g = 1, 2$ genders, and $a = 1, \ldots, n$ age groups, given the observed A_{ga_j} and M_{ga_j}, by minimizing the sum of squared differences between modeled and observed $c_{1a_j 1a_q}, c_{1a_j 2a_q}, c_{2a_j 1a_q}$, and $c_{2a_j 2a_q}$.

2.2.2 Optimal Immunization—Insofar as different endeavors require distinct spaces, which bring people into close proximity, time-use studies complement face-to-face conversations as proxies for contacts by which respiratory diseases might be transmitted. A synthesis of US studies (Zagheni et al. 2008), together with the approach by which Del Valle et al. (2007) convert periods together into contacts, permits us to formulate the simplest transmission model that is capable of informing vaccination policy in age- and location-stratified meta-populations. Using the gradient (partial derivatives of the meta-population effective reproduction number with respect to sub-population immunities or immunization rates), we compare influenza vaccination in the United States from October 2009 through June 2010, assessed via the National 2009 H1N1 Flu Survey (NHFS), with the optimal trajectory for control.

For this application, we consider the $m = 51$ sub-populations (e.g., 50 states and District of Columbia) and $n = 7$ age groups (e.g., 0–9, 10–17, 18–34, 35–44, 45–54, 55–64, 65+ years) in the National 2009 H1N1 Flu Survey (NHFS). Letting l_i denote the i^{th} sub-population and a_j denote the j^{th} age group,

$$\frac{dS_{l_i a_j}}{dt}=\mu N_{l_i a_j}-\left(\chi_{l_i a_j}+\mu+\lambda_{l_i a_j}\right)S_{l_i a_j},\ \ 1 \leq i \leq m\,;\text{and}\,;1 \leq j \leq n$$

$$\frac{dE_{l_i a_j}}{dt}=\lambda_{l_i a_j}S_{l_i a_j}-(\alpha+\mu)E_{l_i a_j}$$

$$\frac{dI_{l_i a_j}}{dt} = \alpha E_{l_i a_j} - (\gamma + \mu) I_{l_i a_j}$$

$$\frac{dR_{l_i a_j}}{dt} = \chi_{l_i a_j} S_{l_i a_j} + \gamma I_{l_i a_j} - \mu R_{l_i a_j}$$

$$\text{where } ; \lambda_{l_i a_j} = A_{l_i a_j} \beta_{a_j} \sum_{p=1}^{m} \sum_{q=1}^{n} c_{l_i a_j l_p a_q} \left[\frac{I_{l_p a_q} \left(1 - \kappa_{l_p a_q}\right)}{N_{l_p a_q}} \right], \ 1 \le i, p \le m, \ ; \text{and} \ ; 1 \le j, q \le n.$$

In this model, people are Susceptible, Exposed (infected, but not yet infectious), Infectious, or Removed (immune by virtue of infection and recovery or immunization). Immunization occurs at rate $\chi_{l_i a_j}$, the product of the vaccination rate and probability of becoming immune, about 77% overall for monovalent H1N1 vaccine (Simpson et al. 2012), $1/\alpha$ and $1/\gamma$ are the latent and recovery (duration of infectiousness) periods (Carrat et al. 2008), β_{a_j} is susceptibility, the probability of infection on contact with an infectious person, of whom the fraction $\kappa_{l_p a_q}$ effectively self-quarantine (e.g., stay home).

2.2.2.1 Effective Reproduction Number: Given that $N = S + E + I + R$, we can eliminate the R equation. Let

$$u_{l_i a_j} = \frac{S_{l_i a_j}}{N_{l_i a_j}}, x_{l_i a_j} = \frac{E_{l_i a_j}}{N_{l_i a_j}}, y_{l_i a_j} = \frac{I_{l_i a_j}}{N_{l_i a_j}}, \ \ i = 1, \ldots, m \ \text{and} \ ; j = 1, \ldots, n.$$

Then the system for the fractions (ignoring the removed class) becomes

$$u'_{l_i a_j} = 1 - \left(\lambda_{l_i a_j} + \chi_{l_i a_j} + \mu\right) u_{l_i a_j}$$

$$x'_{l_i a_j} = \lambda_{l_i a_j} u_{l_i a_j} - (\alpha + \mu) \, x_{l_i a_j}$$

$$y'_{l_i a_j} = \alpha x_{l_i a_j} - (\gamma + \mu) \, y_{l_i a_j}$$

$$\lambda_{l_i a_j} = A_{l_i a_j} \beta_{a_j} \sum_{p=1}^{m} \sum_{q=1}^{n} c_{l_i a_j l_p a_q} \left(1 - \kappa_{l_p a_q}\right) y_{l_p a_q}, \ \ 1 \le i, p \le m \, ; \text{and} \, 1 \le j, q \le n.$$

At the disease-free equilibrium,

$$u^*_{l_i a_j} = \frac{\mu}{\mu + \chi_{l_i a_j}},\ i = 1, ..., m\ ;\text{and}\ ;j = 1, ..., n.$$

Arrange the variables in the order (**x**, **y**), where

$$\mathbf{x} = (x_{l_1 a_1}, x_{l_1 a_2}, \ldots, x_{l_1 a_n}, x_{l_2 a_1}, x_{l_2 a_2}, \ldots, x_{l_2 a_n}, \ldots, x_{l_m a_1}, x_{l_m a_2}, \ldots, x_{l_m a_n})$$

$$\mathbf{y} = (y_{l_1 a_1}, y_{l_1 a_2}, \ldots, y_{l_1 a_n}, y_{l_2 a_1}, y_{l_2 a_2}, \ldots, y_{l_2 a_n}, \ldots, y_{l_m a_1}, y_{l_m a_2}, \ldots, y_{l_m a_n}).$$

Proceeding via the method of van den Driessche and Watmough (2002), the Jacobian at E_0 (considering only the disease variables) is

$$J = \begin{pmatrix} J_{11} & J_{12} \\ J_{21} & J_{22} \end{pmatrix},$$

where J_{ij} are mn by mn matrices with

$$J_{11} = -(\alpha+\mu) I_{mn}, J_{21} = \alpha I_{mn}, J_{22} = -(\gamma+\mu) I_{mn},$$

where I_{mn} is the identity matrix of size $m \times n$ and

$$J_{12} = \begin{pmatrix} A_{l_1 a_1} c_{l_1 a_1 l_1 a_1} \beta_{a_1} (1 - \kappa_{l_1 a_1}) u^*_{l_1 a_1} & A_{l_1 a_1} c_{l_1 a_1 l_1 a_2} \beta_{a_1} (1 - \kappa_{l_1 a_2}) u^*_{l_1 a_1} & \cdots & A_{l_1 a_1} c_{l_1 a_1 l_m a_n} \beta_{a_1} (1 - \kappa_{l_m a_n}) u^*_{l_1 a_1} \\ A_{l_1 a_2} c_{l_1 a_2 l_1 a_1} \beta_{a_2} (1 - \kappa_{l_1 a_1}) u^*_{l_1 a_2} & A_{l_1 a_2} c_{l_1 a_2 l_1 a_2} \beta_{a_2} (1 - \kappa_{l_1 a_2}) u^*_{l_1 a_2} & \cdots & A_{l_1 a_2} c_{l_1 a_2 l_m a_n} \beta_{a_2} (1 - \kappa_{l_m a_n}) u^*_{l_1 a_2} \\ \vdots & \vdots & \ddots & \vdots \\ A_{l_m a_n} c_{l_m a_n l_1 a_1} \beta_{a_n} (1 - \kappa_{l_1 a_1}) u^*_{l_m a_n} & A_{l_m a_n} c_{l_m a_n l_1 a_2} \beta_{a_n} (1 - \kappa_{l_1 a_2}) u^*_{l_m a_n} & \cdots & A_{l_m a_n} c_{l_m a_n l_m a_n} \beta_{a_n} (1 - \kappa_{l_m a_n}) u^*_{l_m a_n} \end{pmatrix}.$$

Let $J = F - V$, where

$$F = \begin{pmatrix} 0 & J_{12} \\ 0 & 0 \end{pmatrix},\ V = \begin{pmatrix} (\alpha+\mu) I_{mn} & 0 \\ -\alpha I_{mn} & (\gamma+\mu) I_{mn} \end{pmatrix},$$

and note that

$$V^{-1} = \begin{pmatrix} \frac{1}{\alpha+\mu} I_{mn} & 0 \\ \frac{\alpha}{\alpha+\mu} \cdot \frac{1}{\gamma+\mu} I_{mn} & \frac{1}{\gamma+\mu} I_{mn} \end{pmatrix}.$$

The next-generation matrix is

$$K:=FV^{-1}=\begin{pmatrix} K_{11} & * \\ 0 & 0 \end{pmatrix}, \text{ where } K_{11}=\frac{\alpha}{\alpha+\mu}\cdot\frac{1}{\gamma+\mu}J_{12},$$

$$=\begin{pmatrix} \Re^{(v)}_{l_1a_1}c_{l_1a_1l_1a_1}(1-\kappa_{l_1a_1}) & \Re^{(v)}_{l_1a_1}c_{l_1a_1l_1a_2}(1-\kappa_{l_1a_2}) & \cdots & \Re^{(v)}_{l_1a_1}c_{l_1a_1l_ma_n}(1-\kappa_{l_ma_n}) \\ \Re^{(v)}_{l_1a_2}c_{l_1a_2l_1a_1}(1-\kappa_{l_1a_1}) & \Re^{(v)}_{l_1a_2}c_{l_1a_2l_1a_2}(1-\kappa_{l_1a_2}) & \cdots & \Re^{(v)}_{l_1a_2}c_{l_1a_2l_ma_n}(1-\kappa_{l_ma_n}) \\ \vdots & \vdots & \ddots & \vdots \\ \Re^{(v)}_{l_ma_n}c_{l_ma_nl_1a_1}(1-\kappa_{l_1a_1}) & \Re^{(v)}_{l_ma_n}c_{l_ma_nl_1a_2}(1-\kappa_{l_1a_2}) & \cdots & \Re^{(v)}_{l_ma_n}c_{l_ma_nl_ma_n}(1-\kappa_{l_ma_n}) \end{pmatrix},$$

$$\text{and } \Re^{(v)}_{l_ia_j}=\frac{\alpha}{\alpha+\mu}\cdot\frac{1}{\gamma+\mu}A_{l_ia_j}\beta_{a_j}u^*_{l_ia_j},\ \ 1\le i\le m \ \text{ and } 1\le j\le n,$$

is the effective reproduction number of the sub-population composed of age-group a_j at location l_i. The '*' denotes a mn by mn block matrix that does not affect the eigenvalues of K. The meta-population $\Re^{(v)}$ is the dominant eigenvalue of K_{11}. If

$c_{l_ia_jl_pa_q}=\frac{A_{l_pa_q}N_{l_pa_q}}{\sum_r\sum_k A_{l_ra_k}N_{l_ra_k}}$, all rows of K_{11} are multiple, so the matrix has rank 1. Consequently, $\Re^{(v)}$ is given by its trace, $\Re^{(v)}=\sum_{i=1}^{m}\sum_{j=1}^{n}\Re^{(v)}_{l_ia_j}c_{l_ia_jl_ia_j}\left(1-\kappa_{l_ia_j}\right)$.

2.2.2.2 Parameter Estimates: We follow Del Valle et al. (2007) in assuming that the number of contacts during any period δt is Poisson with parameter σ. Thus, the probability of no contacts in time interval δt is $\exp(-\sigma\delta t)$ and that of at least one contact is $1-\exp(-\sigma\delta t)$. Using the daily mean durations $T_{a_qa_j}$ of contacts between persons in age group a_q with those in group a_j from Zagheni et al. (2008), the daily numbers of contacts are $C_{a_qa_j}=1-\exp(-\sigma T_{a_qa_j})$. Writing the marginal sum, $A_{a_q}=\sum_{a_j}c_{a_qa_j}$, we first note that people are mobile, whereupon these average over m locations, i.e., $\overline{A}_{a_q}=\frac{1}{m}\sum_{i=1}^{m}A_{l_ia_q}$. Second, we assume that, while people may engage in similar endeavors, they are less likely to do so together (i.e., to make contact) the more distant their locations. Assuming that the activity of an individual aged a_j at location l_i, $A_{l_ia_j}$, is determined not only by his/her age, but also by the distance, ease of travel, … to other locations, $A_{l_ia_j}=\sum_{k=1}^{m}e^{-b_{a_j}d_{l_il_k}}$, whereupon $\overline{A}_{a_q}=\frac{1}{m}\sum_{r=1}^{m}\sum_{k=1}^{m}e^{-b_{a_q}d_{l_rl_k}}$. Thus, if $\overline{A}_{a_q}$ and $d_{l_il_j}$ are known, the b_{a_q} can be estimated for $q=1, 2,\ldots, n$. Given them, we can obtain the $A_{l_ia_j}$ for all age groups at all locations, from which we can obtain $F_{l_ia_j}$, $c^{(p)}_{a_ja_q}$, and $c_{l_ia_jl_pa_q}$ via formulae in two-level example 2.1.2.1, entitled age and location. These formulae ensure that $c_{l_ia_jl_pa_q}\times A_{l_ia_j}\times N_{l_ia_j}=c_{l_pa_ql_ia_j}\times A_{l_pa_q}\times N_{l_pa_q}$.

Influenza vaccine coverage by age and state from October 2009 through June 2010 may be estimated from (http://www.cdc.gov/nchs/nis/data_files_h1n1.htm). We used the responses

of those interviewed during any month to estimate p, the proportion vaccinated that month, with the monovalent H1N1 vaccine. We divided sums of the weights of those vaccinated (the variable VACC_H1N1_F is missing in <1% of records) by sums of all weights in each stratum (state, age group). Then we performed weighted logistic regressions of these estimates by month. From their predicted values, we calculated monthly age- and state-specific vaccination rates, $\chi_{l_i a_j} = -\ln\left[(1-p_{l_i a_j k+1})/(1-p_{l_i a_j k})\right]$, where k and k+1 denote successive months. We also calculated monthly H1N1 vaccine availability from shipments to states from mid-October through mid-January, http://www.cdc.gov/h1n1flu/vaccination/vaccinesupply.htm, less doses administered through the prior month (below).

After converting the daily periods that people spent with others by age from Zagheni et al. (2008) into contacts via the approach of Del Valle et al. (2007), we fitted an interpolating function to the resulting surface, averaged contacts in the n = 7 age groups of the H1N1 coverage data (i.e., 0–9, 10–17, 18–34, 35–44, 45–54, 55–64, 65+ years), and calculated $\overline{A}_{a_q}$. Then we obtained the m = 51 (50 states plus District of Columbia) centroids from *Mathematica*'s geographic database, calculated the inter-state distances, $d_{l_i l_j}$, and solved $\overline{A}_{a_q} = \frac{1}{m}\sum_{r=1}^{m}\sum_{k=1}^{m} e^{-b_{a_q} d_{l_r l_k}}$ for the b_{a_q}. Next, given them and the $d_{l_i l_j}$, we solved $A_{l_i a_j} = \sum_{k=1}^{m} e^{-b_{a_j} d_{l_i l_k}}$; for; the; $A_{l_i a_j}$. And finally, we averaged 2009 and 2010 state populations by age group from CDC Wonder (http://wonder.cdc.gov/population-projections.html) and calculated $c_{l_i a_j l_p a_q} = \frac{A_{l_p a_q} N_{l_p a_q}}{\sum_r \sum_k A_{l_r a_k} N_{l_r a_k}}$. These data, together with monthly vaccination rates and vaccine shipments described above, also enabled us to calculate vaccine administration (by multiplying sums of products of prior monthly vaccination rates and state populations) and, hence, availability.

Fractions seropositive after the second wave of the H1N1 pandemic by age are available from Reed et al. (2012). We fitted the Gamma probability density function, $GF[x;y,z] = \frac{x^{y-1} \times e^{-x/z}}{\Gamma[y] \times z^y}$, to those corrected for immunization (Reed et al., table 2), normalized so that they sum to 1. While $h(a) = \int_0^a GF(x)\,dx$ is an increasing function of age a, we define $f(a) = h(a)/[1+h(a)]$, as the cumulative probability of infection with the 2009 H1N1 pandemic viral subtype at age a. Thus, $f(a) = 1 - e^{-\int_0^a \lambda(x)\,;dx}$ and $\lambda(a) = \frac{d}{da}\{\ln[1+\int_0^a GF(x;y,z)\,dx]\}$. Then we solved $\lambda_{a_j} = \overline{A}_{a_j}\beta_{a_j}\sum_{q=1}^{n} c_{a_j a_q} y_{a_q}$, where y_{a_q} are the proportions seropositive, for the β_{a_j}. Assuming that sub-group sizes remain constant due to balanced inputs and outputs, that α = ½, and γ = ⅓, we calculated $\Re_{l_i a_j}^{(v)} = \frac{\alpha}{\alpha+\mu} \cdot \frac{1}{\gamma+\mu} A_{l_i a_j} \beta_{a_j} u_{l_i a_j}^{*}$, where $u_{l_i a_j}^{*} = \frac{\mu}{\mu+\chi_{l_i a_j}}$, and finally, $\Re^{(v)} = \sum_{i=1}^{m}\sum_{j=1}^{n} \Re_{l_i a_j}^{(v)} c_{l_i a_j l_i a_j}\left(1-\kappa_{l_i a_j}\right)$.

2.2.2.3 Optimal Immunization: As Feng et al. (2015) illustrate for $n = 2$, the gradient describes the most efficient means of attaining any programmatic goal. Their approach involves fixing $\Delta\Re^{(v)}$, the amount by which $\Re^{(v)}$ is to be reduced (assumed small or the prescribed reduction is assumed to be a sum of small increments), and denoting the gradient vector at the point (χ_{1c}, χ_{2c}, …, χ_{mnc}) by $\nabla\Re^{(v)} = (v_{1c}, v_{2c}, \ldots, v_{mnc})$. For ease of notation, re-label the sub-populations with a single index $k = 1, \ldots, mn$. Note that $\Re^{(v)}$ is a decreasing function of χ_k, the immunization rate. Denote this function by $\Re^{(v)}(\chi_1, \chi_2, \ldots, \chi_{mn})$. In the following, we assume that all other parameters are fixed save the χ_k, and use the gradient to determine the optimal immunization strategy, denoted by $(\hat{\chi}_1, \hat{\chi}_2, ..., \hat{\chi}_{mn})$, for reducing $\Re^{(v)}$.

If we increase the immunization rates by ($\Delta\chi_1$, $\Delta\chi_2$, …, $\Delta\chi_{mn}$) along a unit direction, $\vec{u} = (a_1, a_2, ..., a_{mn})$, then $(\Delta\chi_1, \Delta\chi_2, ..., \Delta\chi_{mn}) = r\,\vec{u}$, where r is a constant determining the magnitude of the vector ($\Delta\chi_1$, $\Delta\chi_2$, …, $\Delta\chi_{mn}$). It follows that $\Delta\Re^{(v)} \approx (v_{1c}, v_{2c}, ..., v_{mnc}) \cdot \left(r\,\vec{u}\right)$, so that $\left|\Delta\Re^{(v)}\right| \approx r\,|(v_{1c}, v_{2c}, ..., v_{mnc})| \times |\mathrm{Cos}\Theta|$, where Θ is the angle between the gradient vector at (v_{1c}, v_{2c}, …, v_{mnc}) and the unit length vector $\vec{u}$. Note that the expression $|(v_{1c}, v_{2c}, ..., v_{mnc})| \times |\mathrm{Cos}\Theta|$ is largest when $|\mathrm{Cos}\Theta|=1$ (i.e., when $\Theta = \pi$, because $\partial\Re^{(v)}/\partial\chi_k < 0$). Thus, the value of r is minimized when $\vec{u}$ is parallel to the gradient vector $\nabla\Re^{(v)} = (v_{1c}, v_{2c}, \ldots, v_{mnc})$; that is, $\vec{u} = (v_{1c}, v_{2c}, ..., v_{mnc}) / |(v_{1c}, v_{2c}, ..., v_{mnc})|$. Thus, $(\Delta\chi_1, \Delta\chi_2, ..., \Delta\chi_{mn}) \approx r\,(v_{1c}, v_{2c}, ..., v_{mnc}) / |(v_{1c}, v_{2c}, ..., v_{mnc})|$, whereupon $\Delta\chi_1 N_1 + \Delta\chi_2 N_2 + ... + \Delta\chi_{mn} N_{mn} \approx r\,(v_{1c}N_1 + v_{2c}N_2 + ... + v_{nc}N_n) / |(v_{1c}, v_{2c}, ..., v_{mnc})|$. Therefore, the necessary increase in doses, $\Delta\chi_1 N_1 + \Delta\chi_2 N_2 + ... + \Delta\chi_{mn} N_{mn}$, is smallest when the vector $(\Delta\chi_1, \Delta\chi_2, ..., \Delta\chi_{mn})$ is parallel to the gradient vector $\nabla\Re^{(v)}$ at the point $(\chi_{1c}, \chi_{2c}, ..., \chi_{mnc})$.

The gradient can also be used to devise optimal allocation strategies for vaccines with limited availability, as influenza vaccine typically is early each fall. We can minimize the function $\Re^{(v)}(\chi_1, \chi_2, \ldots, \chi_{mn})$ for fixed total daily doses, $\chi_1 N_1 + \chi_2 N_2 + ... + \chi_{mn} N_{mn} = c$, where c > 0 is a constant representing the doses available and the N_k also are fixed. We solve $\nabla\Re^{(v)} + \lambda\,(N_1, N_2, ..., N_{mn}) = 0$, subject to $\chi_1 N_1 + \chi_2 N_2 + ... + \chi_{mn} N_{mn} = c$, where λ is the Lagrange multiplier. Notice that the constraint corresponds to a “plane” with normal direction parallel to the vector (N_1, N_2, …, N_{mn}). As this plane is orthogonal to $\nabla\Re^{(v)}$ at the solution point $(\hat{\chi}_1, \hat{\chi}_2, ..., \hat{\chi}_{mn})$, its intersection with the contour “surface” of $\Re^{(v)}(\chi_1, \chi_2, \ldots, \chi_{mn})$, to which it is tangent, is the optimal immunization program (figure A1).

3. Results

Our objectives are to develop meta-population modeling methods and to illustrate the utility of the analyses that this approach permits. As meta-population modeling depends on realistic mixing, we began by developing single-level functions with 4 and 5 types of preferential mixing, compared in figure 1, and a generalized multi-level scheme whose proportional mixing formulae are illustrated in figure 2. Subsequent figures illustrate applications of two-

level mixing functions to influenza, an age-gender function that may facilitate reassessment of prolonged school closures and an age-location function with which we illustrate one means of determining the optimal allocation of limited vaccine.

3.1 Theoretical Results

Figures 1 compare our successive 3- and 5-diagonal generalizations of the function of Jacquez et al. (1988), the first to include preferential contacts with parents and children and among co-workers as well as contemporaries and second to include grandparents and grandchildren, but not co-workers. Figures 2 illustrate proportional mixing with respect to age, location, and both in our multi-level scheme. While symbol sizes are the same for older and younger ages, above and below the focal age (denoted by a larger dot in figures 2a and c), respectively, mixing is proportional to products of age-specific contact rates and sub-population sizes (i.e., contacts), which generally will differ among age groups. Similarly, sub-population sizes generally will differ among locations (figures 2b and c).

The 5-diagonal mixing function is our latest generalization of Nold's (1980) function, which Jacquez et al. (1988) modified by allowing the fraction of contacts reserved for others in one's own group (termed preference) to vary among groups, and Glasser et al. (2012) modified by adding preferential contacts between parents and children and among co-workers as well as contemporaries. We added preferential contacts between grandparents and grandchildren and, to facilitate parameter estimation, omitted contacts in the workplace. We believe that our multi-level generalization is the first of its kind. Besides a general scheme, we also provide several two-level examples, age with location or birthplace and gender with age or sexual activity. And we use two of these functions in our applications.

Figure 4 illustrates how the gradient may be used to determine the optimal allocation of limited vaccine in a hypothetical meta-population composed of two age groups at each of two locations. As we can only plot three dimensions, we fix the allocation to one sub-population. In the appendix, we explain this and the elements of which figure 4 is composed, and provide parameter values. We perform this calculation for the $m = 51$ locations and $n = 7$ age groups in the National 2009 H1N1 Flu Survey (NHFS) and illustrate age-specific results for one of these locations, the state of California, in figures 9 and 10.

3.2 Substantive Results

Figures 3a–e illustrate contacts with contemporaries, parents, children, grandparents, and grandchildren estimated by fitting our 5-diagonal mixing function to gender-stratified observations from the PolyMod study. Young and old males and females contact contemporaries of their own gender preferentially, but not middle-aged ones. Mothers have more contacts with daughters, but young fathers contact sons preferentially and older fathers daughters. Females of any age have more contacts with mothers than fathers, while men have more contacts with their mothers than fathers. Differences between genders are most striking in contacts between grandchildren and grandparents. Grandfathers contact grandsons disproportionately and vice versa. Granddaughters have more contacts with grandmothers, but grandmothers contact grandchildren of both genders equally. As ordinates

differ, preferential contacts are summed in figure 3f. Complements of these age-specific sums are distributed proportionately.

Figure 5 illustrates age-specific rates at which contacts decrease with distance. This calculation relies on contacts obtained via the method of Del Valle et al. (2007) from the periods together by age reported by Zagheni et al. (2008) and distances obtained from state centroids available in *Mathematica*. Rates are more or less constant until middle age, after which they increase, ultimately twofold. Evidently older people are much less mobile than younger ones.

Figures 6 illustrate age-specific forces or hazard rates of infection calculated from a Gamma function fitted to proportions seropositive corrected for immunization reported by Reed et al. (2012). Figures 7 and 8b illustrate the widely reported greater susceptibility of children than adults to infection with this influenza virus and their equilibrium prevalence. Figure 8a illustrates contributions to the reproduction number – by virtue of the magnitude and age-distribution of their contacts – an observation that however is not limited to influenza (Glasser et al. 2012). Children are super-spreaders (Lloyd-Smith et al. 2005). Our serology-based $\Re_0 = 2.2$ exceeds case-based ones because of asymptomatic infections (i.e., were case-based $\Re_0 = 1.45$, for example, only about $\frac{2}{3}$ of infections would be symptomatic).

These calculations lead directly to figures 9, which illustrate monthly H1N1 vaccination rates for California and compare age-specific immunization rates during the fall of 2009 with the optimal allocation of limited vaccine for reducing the effective reproduction number. Recall that immunization is the product of vaccination and vaccine efficacy. We estimated, from shipments and prior administration, that 836,900, 3,344,190, and 7,163,650 doses were available for use in CA during October, November and December of 2009, respectively. In figure 10, we compare the October immunization rates to those required to further reduce the effective reproduction number during November, but could of course illustrate these calculations for any state and month.

4. Discussion

Meta-population modeling, in which heterogeneous populations are stratified into homogeneous sub-populations (e.g., age groups, genders, spatial strata), is one approach by which heterogeneity may be represented. Compared with other possible modeling approaches, it preserves the most analytical tractability. Meta-population models enabled Feng et al. (2015) to deduce the consequences of ignoring heterogeneity in factors affecting sub-population reproduction numbers and non-random mixing vis-à-vis efforts to prevent outbreaks of vaccine-preventable diseases in general and Glasser et al. (2016) to deduce the impact of heterogeneity due to personal-belief exemptions to vaccination.

The utility of the meta-population approach depends critically on realistic modeling of the means by which pathogens are transmitted among sub-populations. Accordingly, we generalize a function in which mixing is a convex combination of preferential and proportionate contacts within one and between multiple levels. We derive several two-level mixing examples from our multi-level scheme and, to further illustrate the analytical insights

of which meta-population models are capable, use two of these, age with gender and location, respectively, in applications to pandemic influenza.

First we derive a mixing function with which a proposed pandemic mitigation measure could be thoroughly evaluated. This function resembles that of Glasser et al. (2012), which includes preferential mixing between parents and children as well as among co-workers and contemporaries. However, it also includes grandparents and grandchildren, but not co-workers (figures 1). We estimate gender-specific parameters from face-to-face conversations recorded during the PolyMod study. While patterns of preferential mixing by age and gender are interesting social phenomena, these results motivated us to develop the multi-level scheme whose proportionate mixing functions are illustrated in figures 2.

Age- and gender-specific patterns apparent in conversations from a composite of the eight European countries studied by PolyMod investigators are consistent with everyday experience. Preferential contacts are greater within than between genders at younger and older ages, with most disparities likely due to women living longer than men (e.g., younger and older fathers, respectively, contacting sons and daughters preferentially). Grandparents and grandchildren are the most striking exception. Grandmothers contact grandchildren equitably, but grandfathers and grandsons contact one another disproportionately (figures 3). These age- and gender-specific preferences suggest that our 5-diagonal function provides a reliable basis for investigating school-closure scenarios.

By manipulating the intensity (contact rates, a or A) and pattern of mixing (preferences, ε), one can easily determine analytically, via meta-population effective reproduction numbers, the impact of realistic changes in mixing attendant upon school closures of varying duration. We can deduce the impact of reducing contacts among schoolchildren by any factor. But if their preferential contacts became proportional, this would have much less impact than reducing their marginal contact rates. A $\frac{2}{3}$ reduction in $\varepsilon_{1,2}$, $\varepsilon_{1,3}$, and $\varepsilon_{1,4}$, for example, only reduces $\Re_E$ by about 1%, but a $\frac{2}{3}$ reduction in a_2, a_3, and a_4 reduces it by about 25%. Would children's contact rates be reduced or just reallocated, and if the latter, how? Does this depend on children's ages and for how long schools are closed? Social scientists may assist modelers in formulating realistic scenarios that interest policymakers.

Together with methods illustrated in our application to influenza vaccination, this function also permits investigation of whether the greater incidence of several diseases among members of one gender than the other is due to differential exposure or susceptibility versus gender-specific immune responses (Fish 2008). Antibodies to cytomegalovirus, for example, increase more rapidly with age among females than males. Women who are infected for the first time or who experience reactivations of latent virus or re-infection with new viral strains during pregnancy may infect their developing fetuses. Consequences of congenital infection include spontaneous abortions, stillbirths and neurological and sensory impairments. Understanding gender-specific differences in exposure or susceptibility may help to design strategies for deploying the vaccines currently under development most advantageously.

Both applications of multi-level mixing functions described here involve pandemic influenza, but the second is relevant to vaccine-preventable diseases more generally. Feng et al. (2015) showed that the population-immunity threshold, used by health authorities worldwide to guide and evaluate vaccination efforts, is limited to homogeneous populations. They suggested the multivariate partial derivative of the meta-population effective reproduction number with respect to the sub-population immunities instead, as it is appropriate irrespective of heterogeneity or mixing regime (figure 4). Here we use this quantity, the gradient of multi-variable calculus, together with age- and location-specific mixing, to deduce the optimal allocation of limited H1N1 influenza vaccine in the United States during the fall of 2009.

Patterns that are consistent with everyday experience or prior reports also become apparent in the course of this application. Using another proxy for contact rates, periods engaged in similar endeavors, we discovered that the spatial range of human contacts diminishes after middle age (figure 5), a pattern that Read et al. (2014) also observed in southern China. Using US mixing data (Zagheni et al. 2008), together with proportions having serologic evidence of H1N1 virus infection (figure 6), we determined that children and adolescents were more susceptible than adults (figure 7). We also learned that they experienced more infections and contributed more to the basic reproduction number (figure 8), of which our estimate is somewhat higher than case-based ones, leading to the conclusion that about $\frac{1}{3}$ of H1N1 infections were asymptomatic. While this proportion is often cited, we are not aware of other evidence.

Our use of the gradient to devise optimal immunization strategies is new. In some states (e.g., California), the allocation was nearly optimal for reducing the effective reproduction number (figure 9). In others, even more elderly people were vaccinated than optimal from this perspective. Authorities recommended vaccinating persons at risk of complications, including the elderly. Models can help policymakers to devise such recommendations, which often involve weighing tradeoffs between short- and long-term benefits. Vaccinating elderly people may protect them directly, for example, but vaccinating younger people – who contribute disproportionately to the reproduction number – arguably would protect more elderly ones indirectly, especially if vaccine efficacy declines with age. Using these methods, modelers can also fine-tune public health efforts (figure 10).

5. Conclusions

Meta-population modeling permits one to deduce the consequences of heterogeneity analytically. The utility of this approach depends on the functions by which contacts among the members of sub-populations are modeled. Intermediate results of realistic meta-population models are consistent with everyday experience or observations, reassuring us about the reliability of insights derived for novel circumstances. Such models can help to communicate indirect effects and future benefits to people with different kinds of expertise, most affected by, if not involved in the making of, public health policy.

Acknowledgments

We dedicate our elaboration of methods for meta-population modeling to the late Richard Levins, an extraordinary population biologist who mentored one and inspired all of us. We are grateful to several reviewers for their constructive comments on earlier drafts of the manuscript.

Funding: ZF's research is supported in part by NSF grant DMS-1022758. The sponsor had no role in study design, data collection, analysis or interpretation, or decision to submit this report for publication.

Appendix

A detailed explanation of figure 4, a contour plot of $\Re^{(v)}$ on the 3-D space (χ_1, χ_2, χ_3), the constraint $\chi_1 N_1 + \chi_2 N_2 + \chi_3 N_3 + \hat{\chi}_4 N_4 = c$, and the gradient $\nabla \Re^{(v)}$.

The parameter values are $\mu = 1/(365\times70)$, $\gamma = 0.15$, $\beta = 0.05$, $A_1 = 8$, $A_2 = A_4 = 10$, $A_3 = 12$, $N_1 = N_2 = N_3 = N_4 = 500$, $\kappa_i = 0$, $c = 0.00005$ N, and axis labels are $\chi_k \times 10^{-4}$. For these values, the optimal immunization rates are $(\hat{\chi}_1, \hat{\chi}_2, \hat{\chi}_3, \hat{\chi}_4) = (4.08,\ 5.02,\ 5.88,\ 5.02) \times 10^{-5}$, at which $\Re^{(v)} = 1.47$.

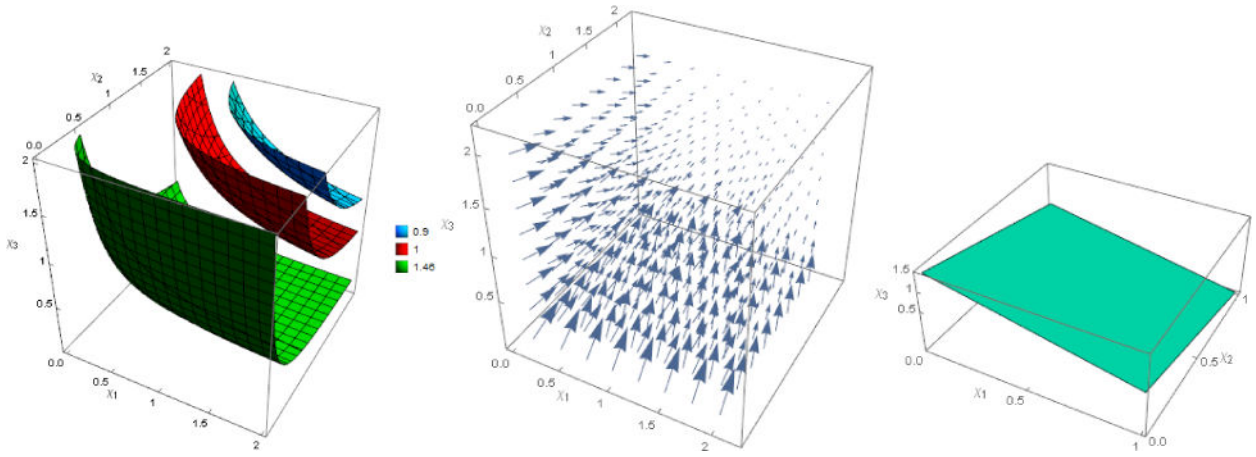

Figure A1.
Separate plots of the elements of figure 4, contour surfaces (left), gradient field (middle), and constraint plane (right).

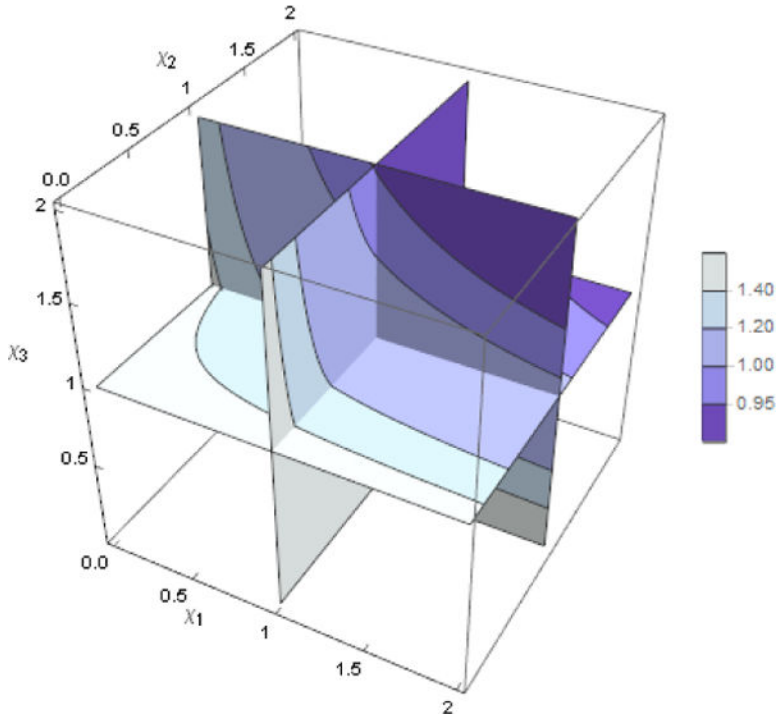

Figure A2.

Contour surfaces in 3-dimensional space for 4 sub-populations shown by slice contour curves in 2-dimensions (a plane) for 3 sub-populations. For a fixed value of χ_2, for example, we can look at the contour curve on the (χ_1, χ_3) plane.

References

Ball F, Britton T, House T, et al. Seven challenges for meta-population models of epidemics, including household models. Epidemics. 2015; 10:63–67. [PubMed: 25843386]

Busenberg S, Castillo-Chavez C. A general solution of the problem of mixing of sub-populations and its application to risk- and age-structured epidemic models for the spread of AIDS. IMA J Math Appl Med Biol. 1991; 8:1–29. [PubMed: 1875096]

Carrat F, Vergu E, Ferguson NM, Lemaitre M, Cauchemez S, Leach S, Valleron A-J. Time lines of infection and disease in human influenza: a review of volunteer challenge studies. Am J Epidemiol. 2008; 167:775–85. [PubMed: 18230677]

Del Valle SY, Hyman JM, Hethcote HW, Eubank SG. Mixing patterns between age groups in social networks. Soc Networks. 2007; 29:539–54.

Feng Z, Hill AN, Smith PJ, Glasser JW. An elaboration of theory about preventing outbreaks in homogeneous populations to include heterogeneity or preferential mixing. J Theor Biol. 2015; 386:177–87. [PubMed: 26375548]

Fish EN. The x-files in immunity: sex-based differences predispose immune responses. Nat Rev Immunol. 2008; 8:737–44. [PubMed: 18728636]

Glasser JW, Feng Z, Moylan A, Del Valle S, Castillo-Chavez C. Mixing in age-structured population models of infectious diseases. Math Biosci. 2012; 235:1–7. [PubMed: 22037144]

Glasser JW, Feng Z, Omer SB, Smith PJ, Rodewald LE. The effect of heterogeneity in uptake of the measles, mumps, and rubella vaccine on the potential for outbreaks of measles: a modelling study. Lancet Infect Dis. 2016; 16:599–605. [PubMed: 26852723]

Hethcote, HW. Modeling heterogeneous mixing in infectious disease dynamics. In: Isham, V., Medley, G., editors. Models for Infectious Human Diseases: Their Structure and Relation to Data. Cambridge University Press; Cambridge, UK: 1996. p. 215-38.

Jacquez JA, Simon CP, Koopman J, Sattenspiel L, Perry T. Modeling and analyzing HIV transmission: the effect of contact patterns. Math Biosci. 1988; 92:119–99.

Levins R. Some demographic and genetic consequences of environmental heterogeneity for biological control. Bull Entomol Soc Am. 1969; 15:237–40.

Lloyd-Smith JO, Schreiber SJ, Kopp PE, Getz WM. Super-spreading and the effect of individual variation on disease emergence. Nature. 2005; 438:355–59. [PubMed: 16292310]

Mossong J, Hens N, Jit M, et al. Social contacts and mixing patterns relevant to the spread of infectious diseases. PLoS Med. 2008; 5:381–91.

Nold A. Heterogeneity in disease transmission modeling. Math Biosci. 1980; 52:227–40.

Read JM, Lessler J, Riley S, et al. Social mixing patterns in rural and urban areas of southern China. Proc R Soc B. 2014; 281:20140268.

Reed C, Katz JM, Hancock K, Balish A, Fry AM, H1N1 Serosurvey Working Group. Prevalence of seropositivity to pandemic influenza A/H1N1 virus in the United States following the 2009 pandemic. PLoS One. 2012; 7(10):e48187. [PubMed: 23118949]

Simpson CR, Ritchie LD, Robertson C, Sheikh A, McMenamin J. Effectiveness of H1N1 vaccine for the prevention of pandemic influenza in Scotland, UK: a retrospective observational cohort study. Lancet Infect Dis. 2012; 12:696–702. [PubMed: 22738894]

van den Driessche P, Watmough J. Reproduction numbers and sub-threshold endemic equilibria for compartmental models of disease transmission. Math Biosci. 2002; 180:29–48. [PubMed: 12387915]

Zagheni E, Billari FC, Manfredi P, Melegaro A, Mossong J, Edmunds WJ. Using time-use data to parameterize models for the spread of close-contact infectious diseases. Am J Epidemiol. 2008; 168:1082–90. [PubMed: 18801889]

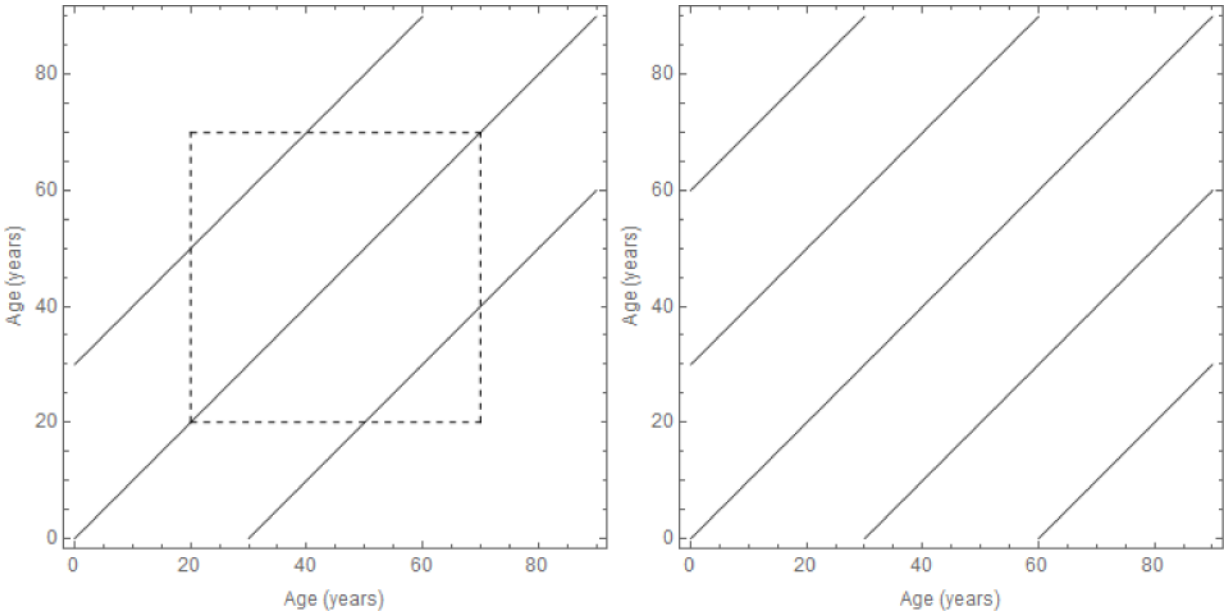

Figure 1.

Generalizations of the function of Jacquez et al. (1988), which allows fractions of contacts to be reserved for one's own group and complements to be distributed proportionally among groups. The age-specific function on the left includes preferential contacts between parents and children (sub- and super-diagonals) and among co-workers (dashed box) as well as contemporaries (main diagonal) while that on the right includes preferential contacts with grandparents and grandchildren (sub-sub- and super-super-diagonals) as well as parents, children and contemporaries.

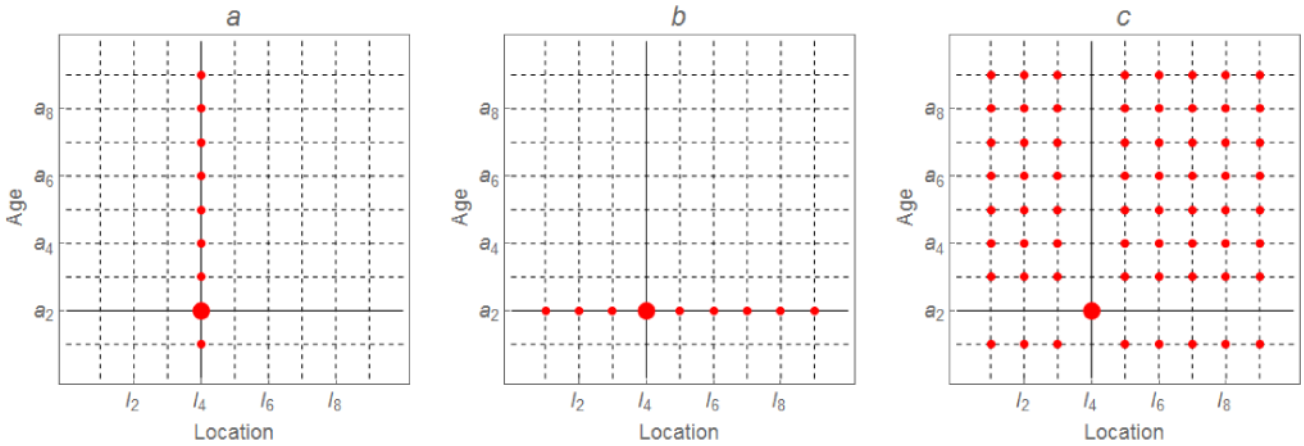

Figure 2.

The functions that describe proportional mixing with respect to one level, F (e.g., age), the other, G (e.g., location), and both, H, in a generalized two-level mixing scheme are illustrated by figures a, b, and c, respectively. By dots of the same size on horizontal lines above and below the large dot in figure a, we do not mean to imply that such mixing is the same from one age group to another. Rather, it is proportional to products of *per capita* contact rates and group sizes, in either or both of which respects groups may differ. Group sizes may vary among locations as well.

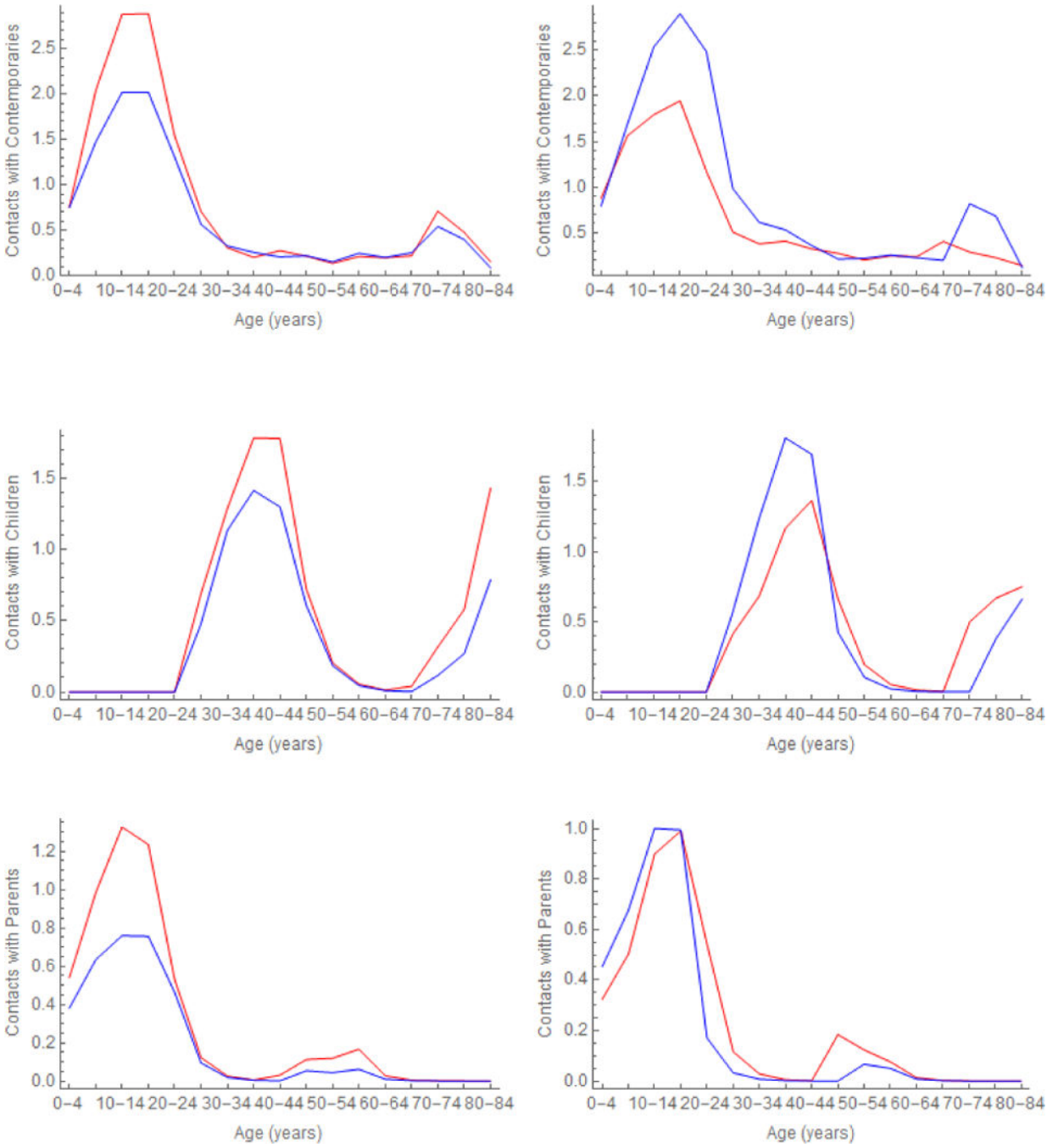

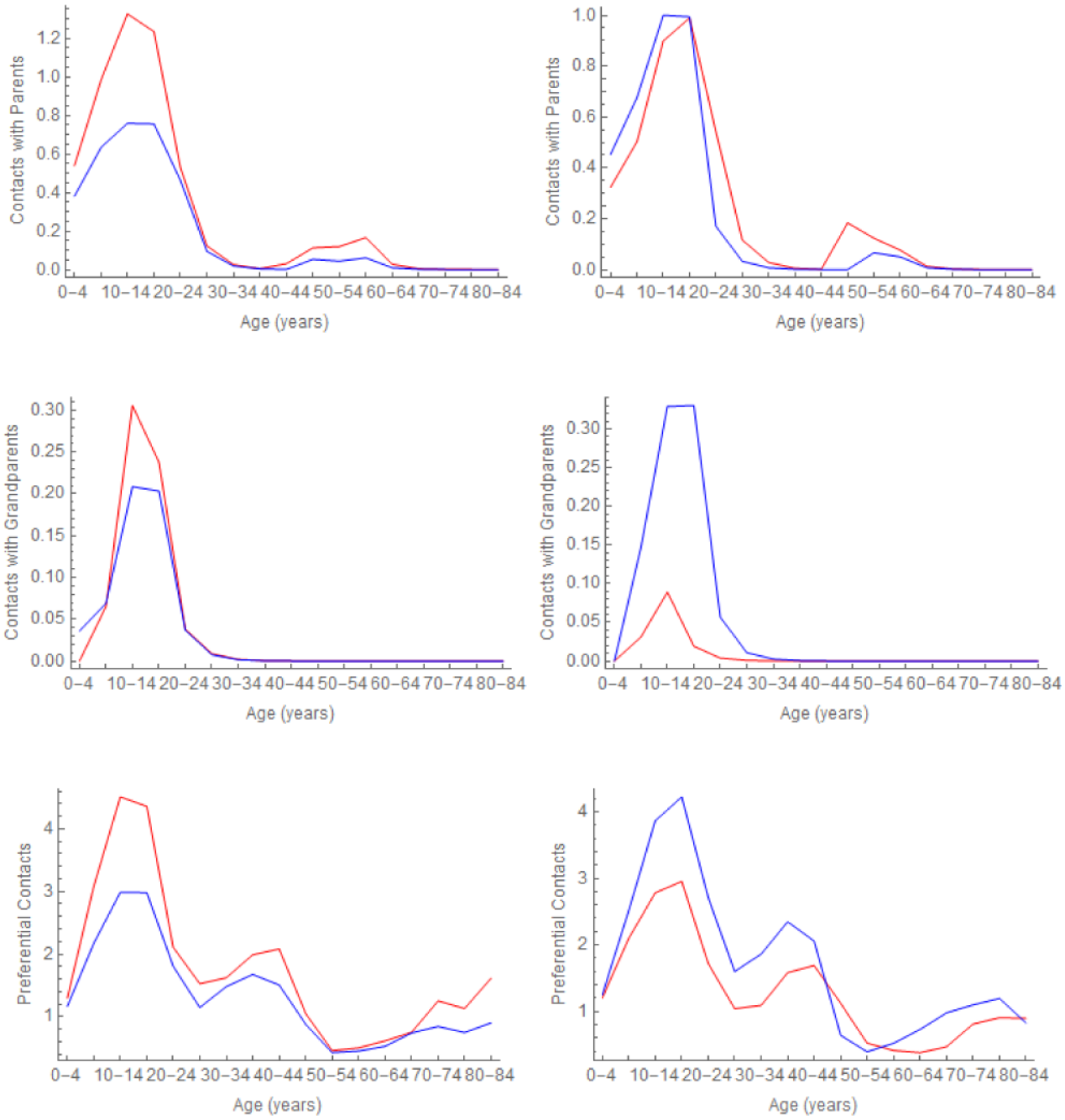

Figure 3.

Estimated age- and gender-specific contacts ($\varepsilon_{sga} \times A_{ga}$) from fitting our 5-diagonal function to gender-stratified observations from the PolyMod study. On the left and right, respectively, are daily contacts by females and males. The red and blue curves, respectively, are their female and male contacts. Thus, the blue curve on the left is female contacts with males. Figures a-e illustrate contacts with contemporaries, children, parents, grandchildren, and grandparents by age, and figure f illustrates all preferential contacts. Ordinates differ top to bottom and, in some cases, left to right.

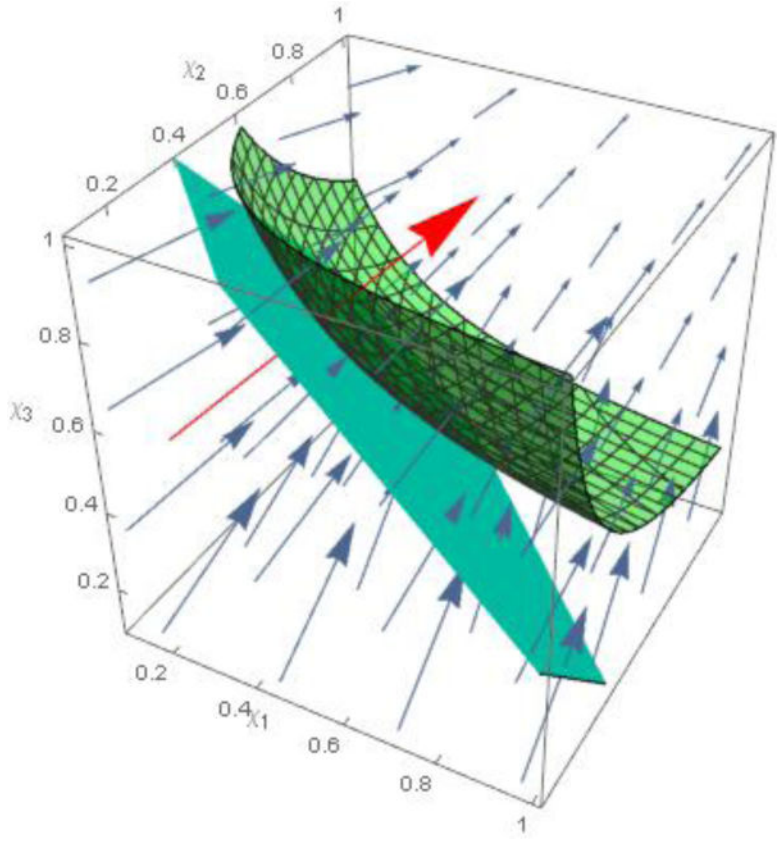

Figure 4.

Contour plot of $\Re^{(v)}$ on the 3-D space (χ_1, χ_2, χ_3) (the curved surface), the constraint $\chi_1 N_1 + \chi_2 N_2 + \chi_3 N_3 + \hat{\chi}_4 N_4 = c$ (the plane), and the gradient $\nabla\Re^{(v)}$ (the arrows). We fix $\hat{\chi}_4 = 5.02 \times 10^{-5}$ and plot $\Re^{(v)}(\chi_1, \chi_2, \chi_3, \hat{\chi}_4)$ as a function of the first three variables. The curved surface is a contour plot of $\Re^{(v)}(\chi_1, \chi_2, \chi_3, \hat{\chi}_4) = 1.47$, the plane is $\chi_1 N_1 + \chi_2 N_2 + \chi_3 N_3 + \hat{\chi}_4 N_4 = c$, and the arrows show the gradient $\nabla\Re^{(v)}$. The optimal allocation $(\hat{\chi}_1, \hat{\chi}_2, \hat{\chi}_3, \hat{\chi}_4)$ occurs where the plane is tangent to the curved surface. The red arrow is the gradient $\nabla\Re^{(v)}$ at this point, the normal direction of the plane. The appendix includes parameter values and further details.

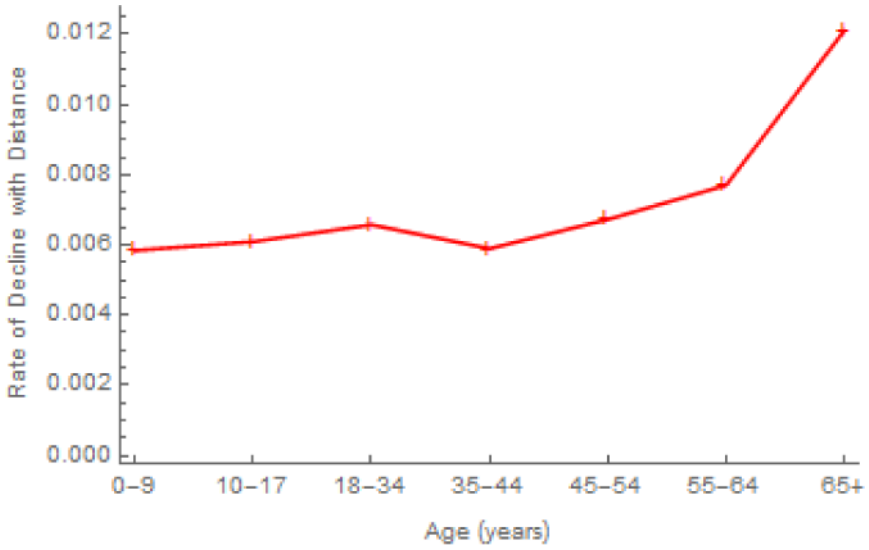

Figure 5.

Age-specific rates at which contacts diminish with distance, b_{a_q}. The doubling of this exponent from youngest to oldest age group indicates a substantial reduction in the spatial range of contacts with age that may warrant consideration insofar as morbidity and mortality are age-dependent.

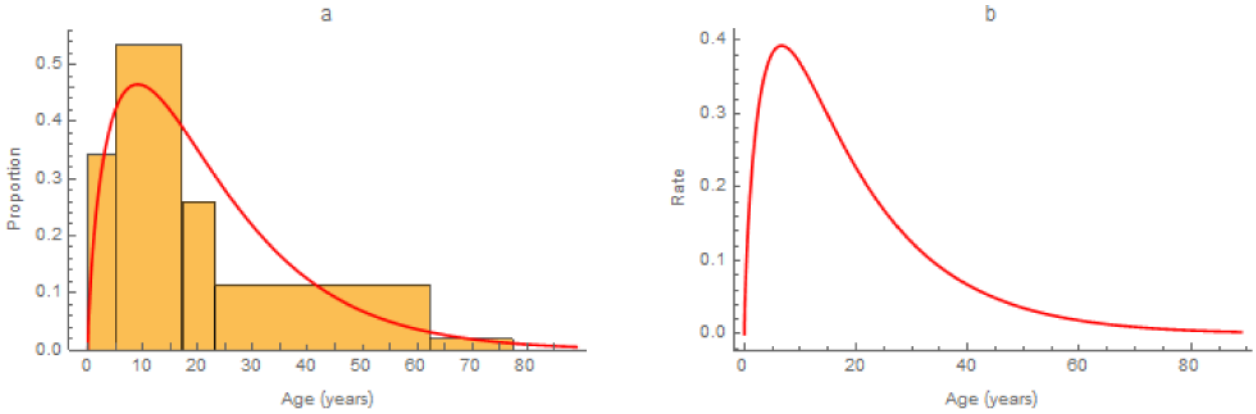

Figure 6.

Observed a) fractions seropositive after the H1N1 pandemic (Reed et al. 2012), less fractions immunized (i.e., fractions infected), fitted Gamma function ($y = 1.68$, $z = 13.16$), and calculated b) force or hazard rate of infection among susceptible people by age.

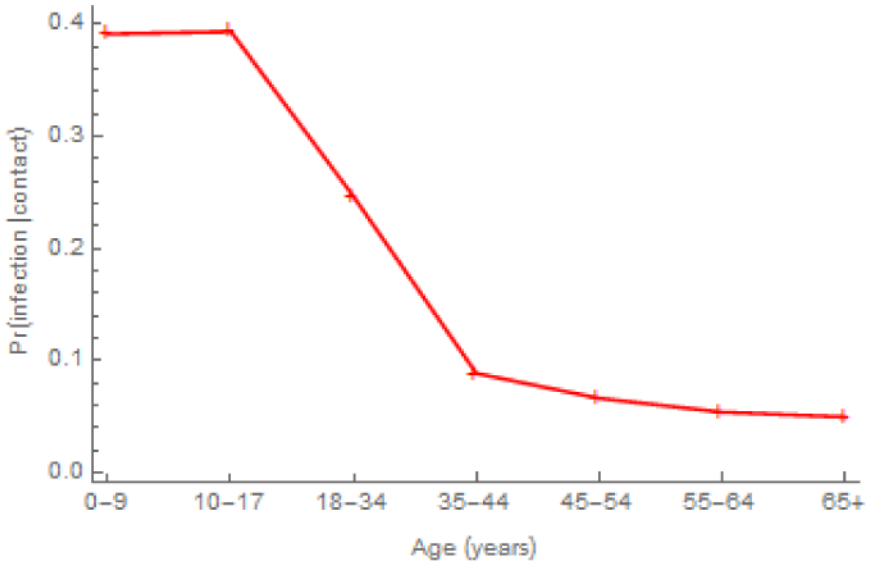

Figure 7.

Probabilities of infection on contact with an infectious person (susceptibility) by age as grouped in the National 2009 H1N1 Flu Survey (NHFS). The decreased susceptibility of older people has been attributed to their exposure to a related virus when younger.

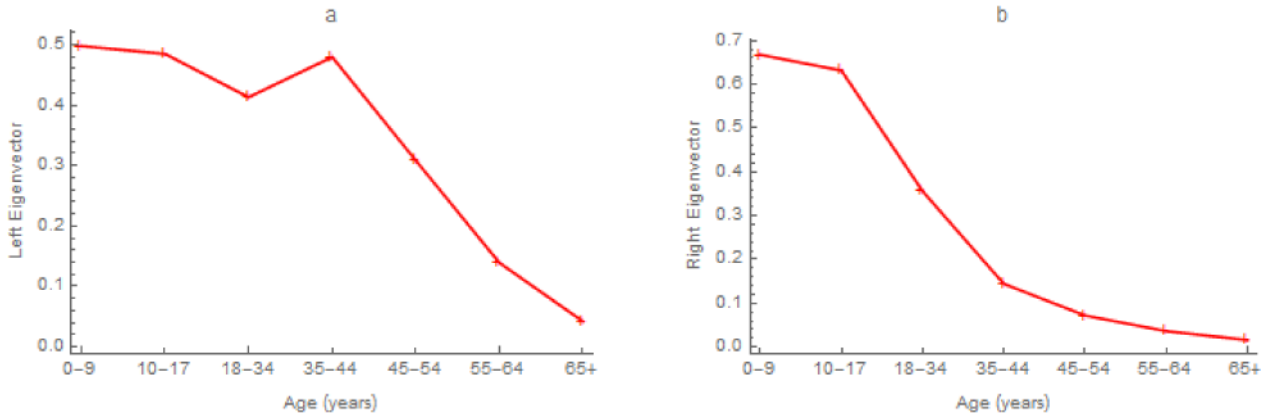

Figure 8.

Eigenvectors associated with the dominant eigenvalue of the next generation matrix, interpretable as age-specific a) contributions to the basic reproduction number and b) equilibrium prevalence. Control measures targeting groups that contribute the most have the greatest impact.

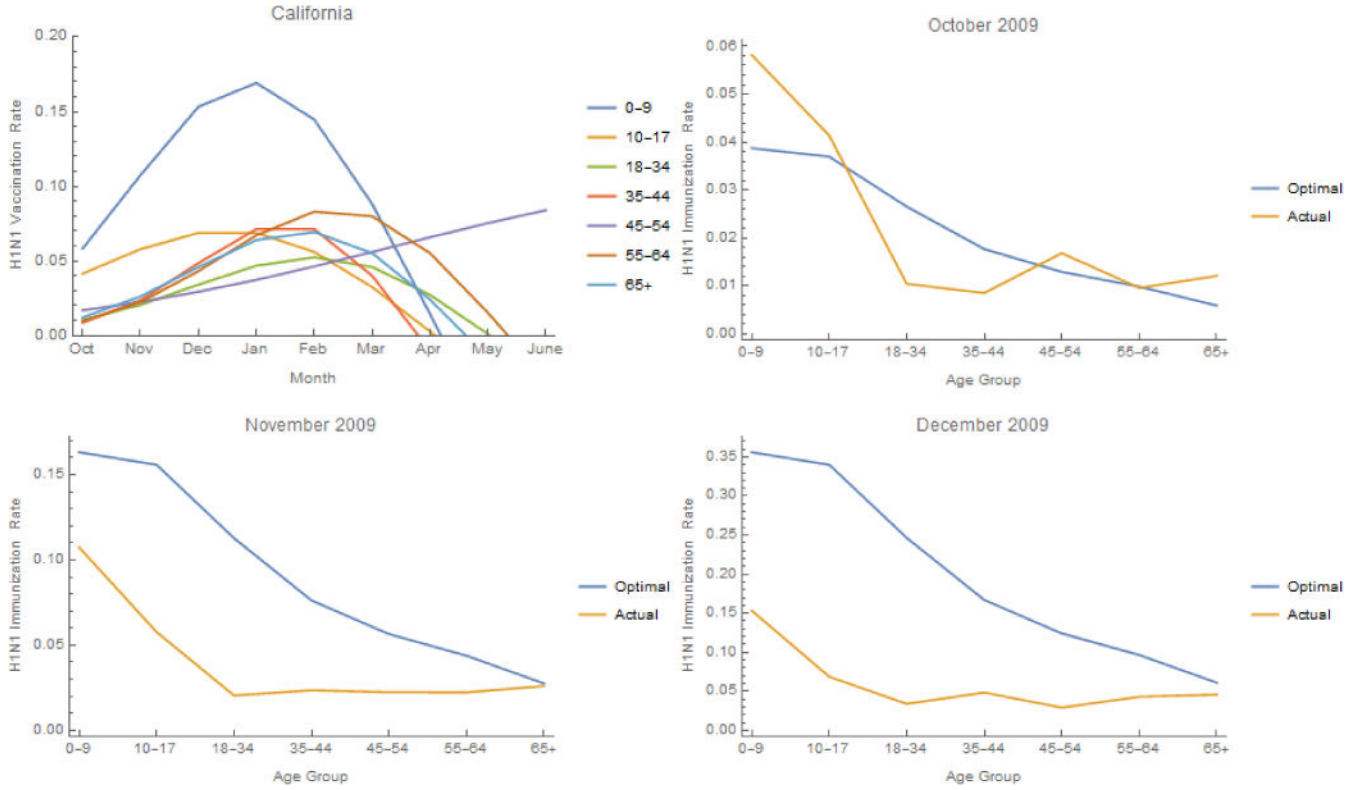

Figure 9.

Calculated H1N1 immunization rates a) by age and month in California and b-d) comparison of the observed and optimal age-specific rates during October (given the 836,900 doses available), November (given the 3,344,190 doses available) and December of 2009 (given the 7,163,650 doses available). Rates peak from late 2009 through early 2010 and corresponded reasonably well to the optimal age distribution when vaccine was scarce, with the exceptions noted in the next figure, but diverged increasingly as more vaccine became available.

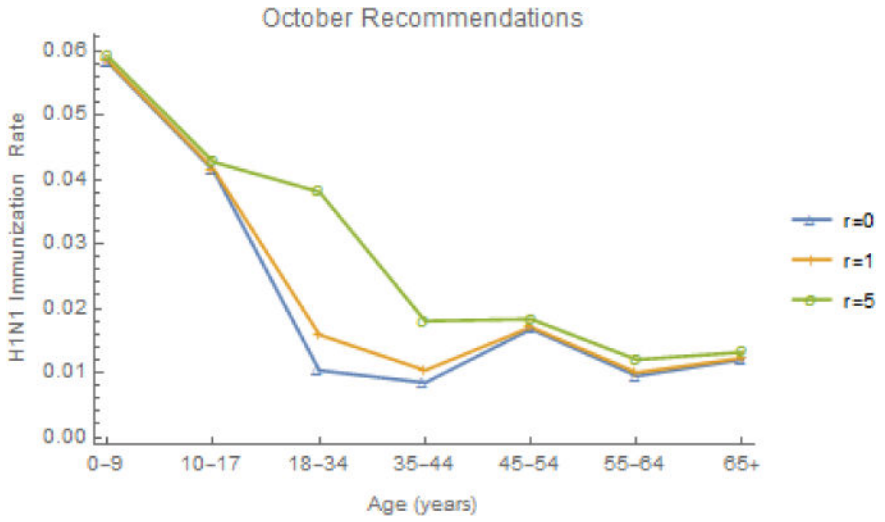

Figure 10.

Increments in California's October 2009 immunization rates that would reduce the effective reproduction number during November by multiples ($r = 0, 1, 5$) of the gradient. The actual rates are denoted by the $r = 0$ line. The magnitude of the gradient is greatest in those age classes where vaccination is sub-optimal, as indicated by figure 9b.